Seismic Performance of Wall-type RC Bridge Piers Retrofitted with AFRP sheet

by

Kenji IKEDA[1)], Hisashi KONNO[2)] , Akira HATAKEYAMA[3)]

ABSTRACT

The introduction of performance evaluation standards that leave great latitude to design method is expected to prompt active use of new construction methods and technologies.

This study aims to develop a design that prevents brittle failure and enhances ductility of the cutoff point of main reinforcement for wall-type RC bridge piers. A seismic retrofit method is proposed in which aramid fiber reinforced plastic (AFRP) sheets are used together with crossing steel bars. To establish a rational seismic retrofit method, basic data were collected through cyclic loading tests using as parameters the exist of flexural reinforcement, shear reinforcement and amounts of AFRP sheet reinforcement.

KEY WORDS：AFRP Sheets
Crossing steel bar
Loading Test
Wall-type RC Bridge Pier

1.INTRODUCTION

The 1995 Hyogo-ken Nanbu Earthquake damaged many RC bridge piers. Brittle failure modes observed at the cutoff point of main reinforcement for many RC piers included flexural/shear or shear.

Various horizontal cyclic loading tests revealed the following:

1) An RC pier with a cutoff point of main reinforcement exhibits brittle failure in which flexural failure progresses to shear failure of the cutoff point.

2) Shear failure can be effectively reduced by enhancing the shear capacity of cutoff point using AFRP sheet.

3) When strength of pier greatly increased, damage progressed to the footing.

Based on these results, static cyclic loading tests were conducted to establish a more efficient retrofit method, using a quarter-scale model of an RC pier. Exist of flexural reinforcement, shear reinforcement and amounts of AFRP sheet reinforcement were the parameters.

2. OUTLINE OF EXPERIMENT

2.(1) Experimental Method

Figure 1 shows a schematic diagram of the experimental device.

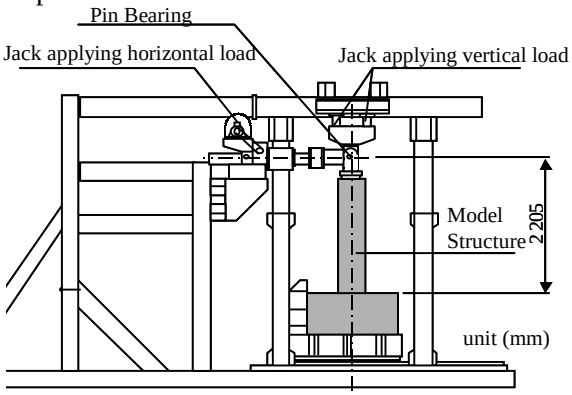

Figure1. Experimental Device

1)Head, Structure Divisions, Structures Department, Civil Engineering Research Institute of Hokkaido, Hiragishi 1-3, Toyohira-ku, Sapporo, Japan

2)Chief Researcher, Structure Divisions, Structures Department Civil Engineering Research Institute of Hokkaido , Hiragishi 1-3, Toyohira-ku, Sapporo, Japan

3)Researcher, Structure Divisions, Structures Department, Civil Engineering Research Institute of Hokkaido , Hiragishi 1-3, Toyohira-ku, Sapporo, Japan

It consists of a jack that applies a vertical load corresponding to the dead load of superstructure, a jack that applies horizontal cyclic loads, the model structure and a frame.

A vertical load of 88.2 kN corresponding to the dead load of the superstructure was applied. Under the constant condition, cyclic loads were applied in the horizontal direction. In addition, pin joint was adopted for the jack sections and the pier crown in order to reproduce the rotation of bearings of an actual bridge.

The cyclic loading test was conducted as follows:

Yield strain of axial reinforcement was set as 1750 μ, based on the results of a material test. Loading point displacement at the time when reinforcement strain at the cutoff point or at the column bottom reached the yield strain was used as yield displacement (δ y), while using the load at that time as yield load (Py). Cyclic loads were applied by gradually increasing the displacement amplitude (for example, 2 δ y, 3 δ y...).

The cycles numbered three for each amplitude. Ultimate state was defined as displacement amplitude of less than Py under either push or pull first loading.

2.(2) Model Structure

We used model structures of about one-quarter scale of an actual wall-type bridge pier that has a cutoff point of axial reinforcement, which is common in existing bridges.

The model structure had a height of 2.0 m and a rectangular cross section of 0.38×1.14 m (side length ratio of 1 : 3). The cutoff point of axial reinforcement was 0.9 m above the column bottom.

The ratio of main reinforcement to tension reinforcement at the column bottom was Pt = 0.6%, and the volume ratio of lateral confining reinforcement was ρ s = 0.14%.

In this experiment, to verify reinforcing effects

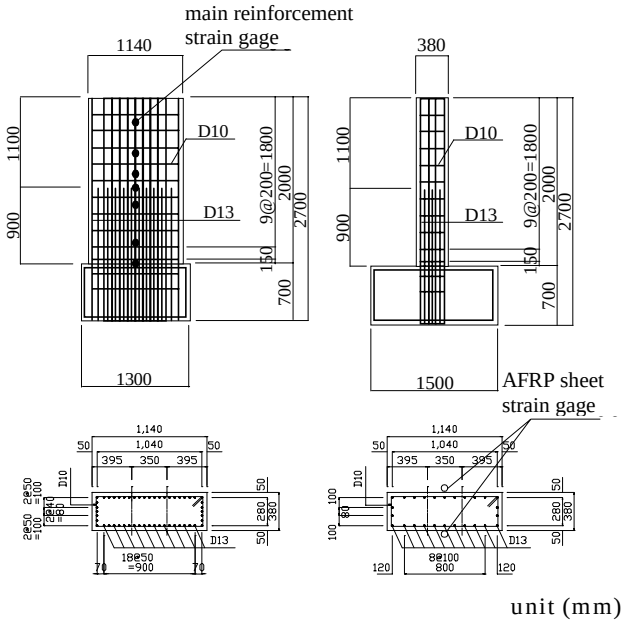

unit (mm)

Figure2. Model Structure Configuration and Dimensions

at the cutoff point, the model structure was designed so that flexural failure would occur first.

Average compressive strength of concrete at the time of experiment was 26.8 MPa for N, A1 and A2, and 25.2 MPa for A3 and A4. Average yield strength of reinforcing bars was 366 MPa.

Figure 2 shows the configuration and dimensions of the model structure.

Strengthening used AFRP sheet, which affords superior workability. Shear and flexural strengths were increased to prevent brittle failure of the cutoff point of main reinforcement and to enhance ductility.

Five model structures were prepared, focusing on 1) shear reinforcing effect of the cutoff point (A1), 2) combined effect of shear and flexural reinforcement of the cutoff point (A2), and 3) combined effect of the reinforcement of the cutoff point (shear reinforcement and flexural reinforcement) and shear reinforcement of the column bottom (A3 and A4). A non-reinforced control structure N also was prepared.

Table1. Reinforcement of Model Structures

model structure	reinforcement range	reinforcement amount (AFRP Sheet)	
		shear reinforcement	flexural reinforcement
N	—	—	—
A1	cutoff point	AK-40 2 layers	—
A2	cutoff point	AK-40 1 layers (bidirectionally woven AFRP sheet)	
A3	cutoff point	AK-40 1 layers (bidirectionally woven AFRP sheet)	
	column bottom	AK-40 1 layers	—
A4	cutoff point	AK-10 2 layers (bidirectionally woven AFRP sheet)	
	column bottom	AK-40 1 layers	—

Table 1 lists the model structures.

The design of shear reinforcement amount was conducted under the assumption that the AFRP sheets act independently in resisting the shearing force acting on the model structure.

Concerning flexural reinforcement of the cutoff point, the value of bending moment of this point when the bending moment of the column bottom reached the ultimate value served as the standard. The flexural reinforcement was designed so that the cutoff point could maintain a resisting moment 1.1 times this standard for A4, and 1.4 times this standard for A2 and A3. AFRP sheets used in the experiment had tensile capacity of 400 kN/m (AK-40) and 100 kN/m (AK-10), an elastic modulus of 118 Gpa and a tensile strength of 2.06 Gpa.

In simultaneously enhancing flexural and shear capacity of the cutoff point, bidirectionally woven AFRP sheet was used to reduce the number of steps for construction and to make construction more efficient.

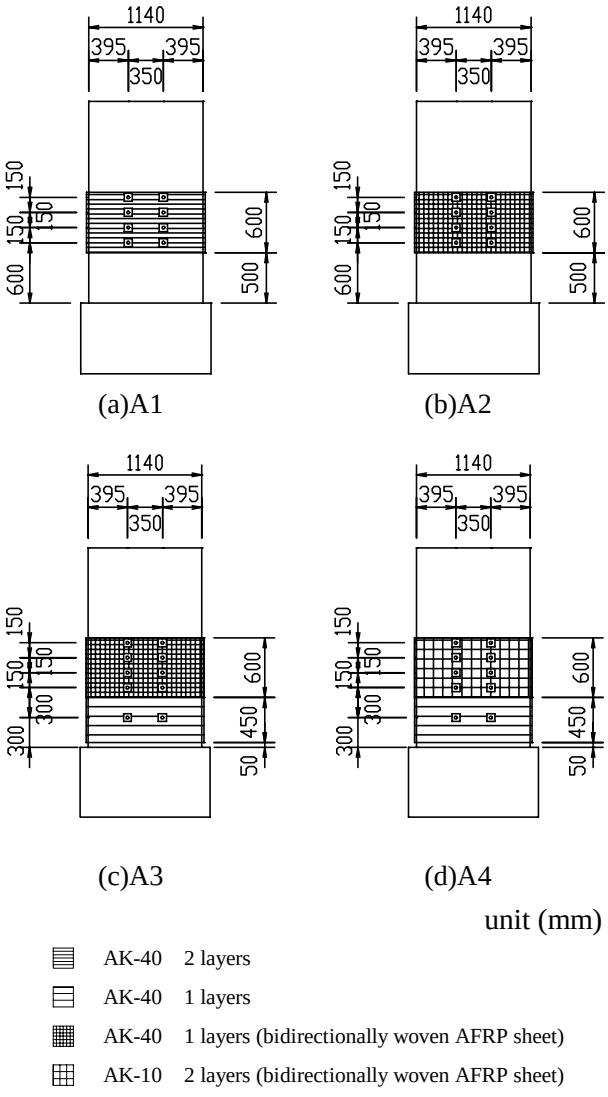

Figure3. Reinforcement of ModelStructures

As the model structure had a rectangular section (side to length ratio of 1 : 3), there was a possibility that AFRP sheet would slacken on the longer side of the pier, and that the confining effect would be insufficient. To address this, crossing steel bars were arranged in two rows. The spacing between crossing steel bars in the height direction was 150 mm at the cutoff point and 300 mm at the column bottom.

Figure 3 shows the reinforcement of the model structures.

Table2. Experimental Results

model structure	displacement(mm)		Load(kN)		ultimate ductility factor
	δ y	δ u	Py	Pu	
N	27.3	102.0	134.55	93.39	4 δ y
A1	19.3	162.5	135.73	122.79	8 δ y
A2	17.8	124.5	125.24	116.62	7 δ y
A3	18.5	131.5	139.94	133.77	7 δ y
A4	21.8	166.5	140.63	128.67	8 δ y

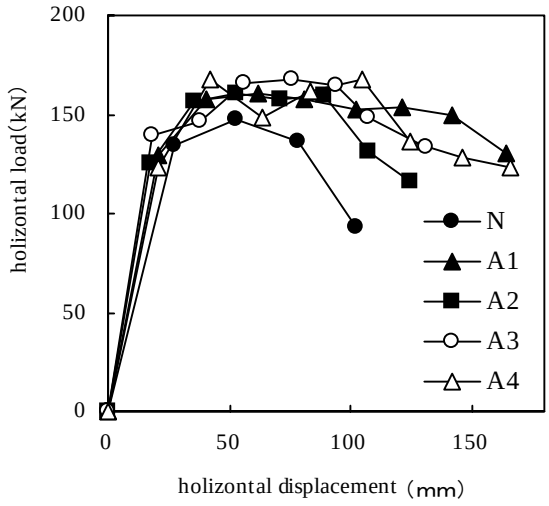

Figure4. Load Displacement Envelope

3.EXPERIMENTAL RESULTS AND DISCUSSION

3. (1) Load-Displacement Relationships

Table 2 shows the experimental results. δ y and Py in the table represent the loading point displacement and the applied load, both at yield. δ u and Pu represent the loading point displacement and applied load, both at ultimate point.

This table shows that as a result of the improvement in rigidity by reinforcement, the yield displacement of each reinforced structure was 20 to 35% smaller than that of model structure N (non-reinforced), while the ultimate displacement was 22 to 63% larger, which indicated that the ductility was greatly enhanced by reinforcement.

Figure 4 shows the load displacement envelope under loading on the push side in one loading loop for each model structure. In the case of model structure N (non-reinforced), after the load peaked at 2 δ y, it rapidly decreased and reached the ultimate state. The reinforced model structures tended to have very little change in load from 2 δ y to 5 δ y, after which the load decreased gradually. The ultimate ductility factor of model structures A2 and A3 was 7 δ y, and that of A1 and A4 was 8 δ y. When the flexural reinforcement amount in the cutoff point of main reinforcement was increased, fairly small values were exhibited.

3.(2) Failure Characterisitcs

Figure 5 shows the failure characteristics of model structures (side view).

- Model structure N (non-reinforced)

After horizontal cracks spread to the sectional center near the cutoff point beneath the load, 1 δ y, shear cracks occurred diagonally downward. After this loading, shear cracking was dominant, and exfoliation of the covering concrete resulted in the ultimate state at 4 δ y. At 1 δ y, flexural cracks occurred near the column bottom, but they were not observed to progress.

- Model structure A1

Flexural cracks at the cutoff point progressed up to 3 δ y, after which cracks also appeared at the column bottom. At the bottom, exfoliation of the covering concrete progressed at 8 δ y, and tearing of AFRP sheet was observed near the anchorage of the crossing steel bar.

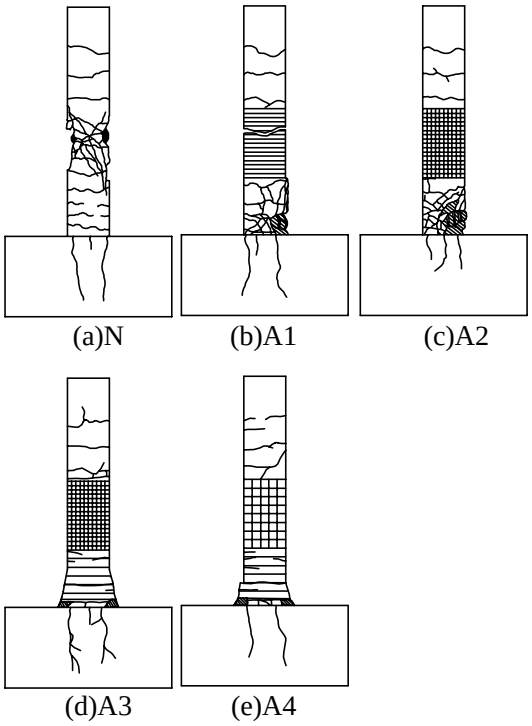

Figure5. Failure Characterisitics of Model Structure

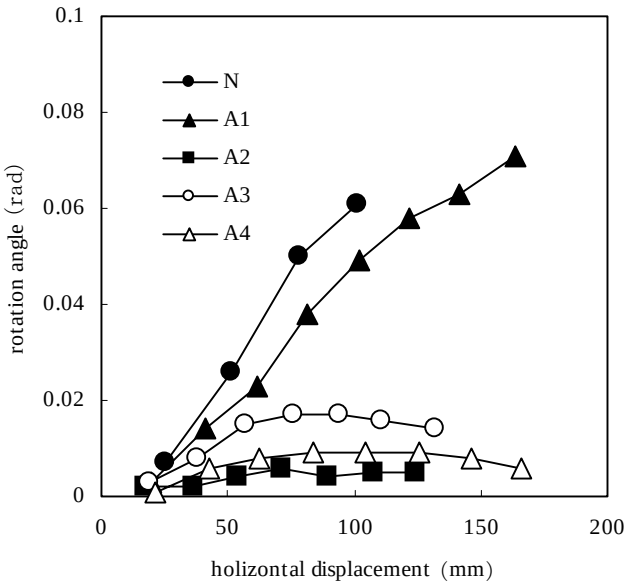

Figure 6. Rotation Angle of Member at the Cross Section of the Cutoff point of Main Reinforcement

- Model structure A2

Damage concentrated at the column bottom from the early stage of loading. The covering concrete there suffered considerable exfoliation, resulting in the ultimate state at 7 δ y. There was no major damage in the AFRP-reinforced section.

- Model structure A3

Damage progressed at the column bottom, and the AFRP sheet detached 30 cm above the base. The AFRP sheet tore at 7 δ y, near the anchorage of the lowest crossing steel bars, and the sheet below the crossing steel bar detached over a large area. In addition, as in the case of model structure A2, damage to the reinforced section was minor.

- Model structure A4

Damage progressed at the column bottom, and the AFRP sheet detached 30 cm above the base. The sheet separated far from the pier in the section below the crossing steel bars mentioned above, but damage to the reinforced section near the cutoff point was not serious.

3.(3) Relationship between Rotation Angle of Member and Horizontal Displacement

Figure 6 shows the relationship between the rotation angle of member and the horizontal displacement at the cross section of the cutoff point.

Figure 6 indicates that model structure N and model structure A1, neither of which was flexurally reinforced at the cutoff point, have large values of rotation angle with increase in horizontal displacement. The rotation angle of model structure N at ultimate displacement was 0.06 rad, and the angle of A1 is 0.08 rad. This suggests that the rotation angle at ultimate

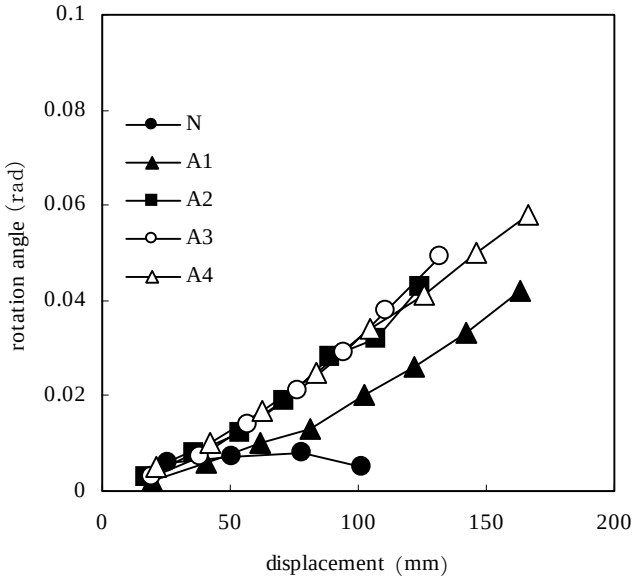

Figure 7. Rotation Angle of Member at the Cross Section of the Column bottom

displacement increased because of the confining effect of core concrete produced by the shear reinforcement of the cutoff point.

As for model structures A2, A3 and A4, which were flexurally reinforced at the cutoff point, the rotation angle does not increase after $3\delta y$, and even the largest value of angle is less than 0.02 rad. These facts suggest that flexural reinforcement at the cutoff point is effective.

Figure 7 shows the relationship between the rotation angle of member and the horizontal displacement at the cross section of the column bottom.

- Model structure N

The rotation angle does not increase with the displacement, which indicates that the deformation of the cutoff point is dominant.

- Model structure A1

The rotation angle greatly increases under the loads after $4\delta y$, and is 0.04 rad at ultimate displacement. This is because exfoliation of the covering concrete at the cutoff point was reduced as a result of the shear reinforcement. The failure mode also shows that the shear reinforcement reduced the exfoliation.

- Model structures A2, A3 and A4 (flexurally reinforced at the cutoff point)

The increase in rotation angle with the increase in horizontal displacement for these three model structures plots as lines of roughly the same slope. Comparison with the angles at the cross sections of the cutoff point and column bottom reveals that the deformation of cutoff point is reduced and the deformation of column bottom is dominant.

Compared with A2 (no shear reinforcement near the column bottom), model structures A3 and A4 (shear reinforcement) exhibit fairly large values of rotation angle at ultimate displacement. A2, A3 and A4 showed maximum values of about 0.04 rad, 0.05 rad and 0.06 rad, respectively. Although A3 and A4 were provided with shear reinforcement, the above values are roughly equal to the value of the rotation angle of model structure N at the cross section of the cutoff point. This means that the AFRP sheet does not display sufficient confining effect.

This may be attributed to the following.

- Because the interval in the height direction between crossing steel bars in the pier is twice that between the crossing steel bars at the bottom, AFRP sheet detached severely below the crossing steel bars, for A3 and A4.
- The sheet partially fractured at the anchorage end of the crossing steel bar (A3).

Consequently, the crossing steel bar arrangement is seen to be important in shear reinforcement of wall-type bridge piers.

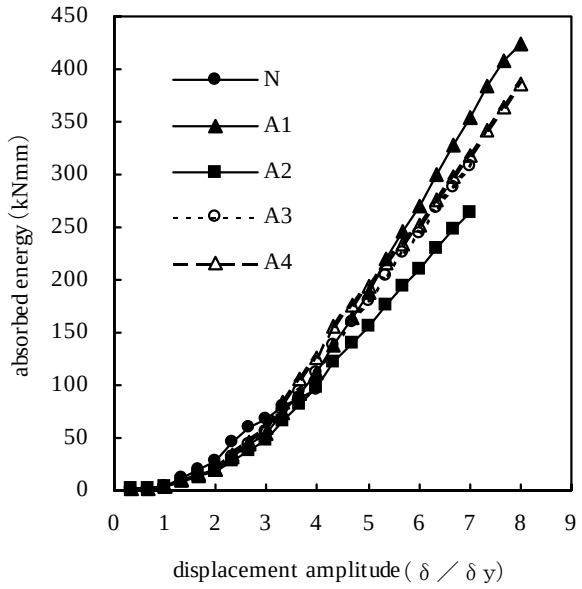

Figure 8. Hysteretic Absorbed Energy

3.(4) Hysteretic Absorbed Energy

Figure 8 shows the relationship between the hysteretic absorbed energy and the displacement amplitude. This absorbed energy was calculated by the relationship between the load and the displacement at each displacement amplitude. **Figure 8** gives cumulative values.

Although the model structures do not differ significantly in the amount of absorbed energy at 4 δ y when the ultimate state is reached in model structure N, dispersion is observed among the model structures under loads after 4 δ y.

The cumulative values of hysteretic absorbed energy up to ultimate state are as follows: N: 95.3 kNmm, A1: 424.5 kNmm, A2: 264.7 kNmm, A3: 307.5 kNmm, A4: 385.2 kNmm.

The reinforced model structures exhibits energy absorption performance 2.7 to 4.5 times those without reinforcement. A1 has the largest value of reinforced model structures. This is probably because A1 is not provided with flexural reinforcement of the cutoff point and, as a result, plastic hinges formed at the cutoff point and at the column bottom.

Among the model structures with flexural reinforcement of the cutoff point, A3 and A4 exhibit almost the same values up to 7 δ y, at the ultimate state in A3. They also show greater energy absorption than A2, which is without the shear reinforcement of the column bottom.

4. Conclusion

Focusing on a retrofit method using AFRP sheets and crossing steel bars, the cyclic loading test were conducted by changing the amount and items of reinforcement, using a quarter-scale model of an actual bridge. The test results are summarized as follows:

1) Damage to the cutoff point of main reinforcement can be effectively reduced by providing the cutoff point with shear and flexural reinforcement, using AFRP sheet and crossing steel bars.

2) When the flexural resistance of the cutoff point is enhanced, the deformation of the column bottom becomes dominant. By enhancing the shear capacity of the column bottom, the energy absorption can be increased. In this experiment, the confinement afforded by AFRP sheet was ineffective, because the crossing steel bars used in the lowest section were positioned too high. The crossing steel bar arrangement is important.

3) When only the shear capacity of the cutoff point is enhanced, the energy absorption performance greatly improves. This is probably because damage progressing near the cutoff point and at the column bottom results in energy being absorbed at two places.